

Phonon-induced dynamic resonance energy transfer

James Lim,^{1,2,3} Mark Tame,^{4,*} Ki Hyuk Yee,^{1,2} Joong-Sung Lee,^{1,2} and Jinhyoung Lee^{1,2,†}

¹*Department of Physics, Hanyang University, Seoul 133-791, Korea*

²*Center for Macroscopic Quantum Control, Seoul National University, Seoul 151-742, Korea*

³*Research Institute for Natural Sciences, Hanyang University, Seoul 133-791, Korea*

⁴*EXSS, The Blackett Laboratory, Imperial College London, Prince Consort Road, SW7 2BW, United Kingdom*

(Dated: December 3, 2024)

In a network of interacting quantum systems achieving fast coherent energy transfer is a notoriously challenging task. While quantum systems are susceptible to a wide range of environmental factors, in many physical settings their interactions with quantized vibrations, or phonons, of a supporting structure are the most prevalent. This leads to noise and decoherence inside the network, ultimately impacting the energy-transfer process. In this work, we introduce a fundamentally new type of coherent energy-transfer mechanism for quantum systems, where phonon interactions actually enhance the energy transfer. Here, a shared phonon interacts with the systems and dynamically adjusts their resonances, providing remarkable directionality combined with quantum speed-up. We call this mechanism phonon-induced dynamic resonance energy transfer and show that it enables long-range coherent energy transport even in highly disordered systems.

PACS numbers: 87.15.hj,05.60.Gg,71.35.-y,63.20.kk

Quantum systems exhibit many features that are contradictory to conventional classical systems. One of the most well known is the concept of wave-particle duality, where a quantum system is able to display both wave-like and particle-like properties. Such nonclassical behavior enables quantum systems to outperform classical systems for a wide range of tasks in information processing and communication [1]. In particular, in energy transport, quantum coherence enables a system to exploit the dynamics of quantum walks [2], which are significantly faster than those of classical walks and diffusion. However, despite the many advantages offered by quantum systems, they are extremely challenging to isolate and invariably interact with their environment. This causes the loss of their wave-like properties by decoherence, ultimately destroying any quantum advantage. In this work, we show that when quantum systems in a network are designed to interact with their environment in a shared way [3], they are able to maintain their quantum coherence and even use it for achieving fast coherent energy transfer via quantum walk dynamics that are highly robust to disorder.

We consider quantized vibrational modes, or phonons, which are carriers of heat widely regarded as forming one of the most dominant mechanisms that reduces coherent effects in many physical systems. In energy transport, for instance, electronic excitations of molecules (excitons) move downhill in energy through dipole-coupled molecules, while their wave-like behavior diminishes rapidly by relaxation into a large number of phonon modes [4]. Here, the incoherent transfer of an exciton has previously been investigated with a shared phonon bath where different molecules are coupled to the same phonon modes [5]. However, recent advances in experimental techniques have made it possible to observe more complex behavior in the quantum regime for engineered structures [6] and biological systems [7]. For a shared phonon bath, coherent transfer of an exciton has been investigated in the equilibrium regime, $\gamma \gg J$, where the relaxation rate γ of phonons to an equilibrium state is faster than the dipole coupling J between molecules responsible for the exciton transfer [8]. Coherent exciton transfer has also been studied for

the case that $\gamma \approx J$ where the phonons relax from a nonequilibrium to an equilibrium state during the exciton transfer [9]. The nonequilibrium behavior of phonons has also been considered in the internal electron transfer in a molecule [10]. In contrast to these earlier studies, here we investigate the exciton transfer through a chain of molecules in the nonequilibrium regime, $\gamma \ll J$, where the shared phonon is in a nonequilibrium state during the exciton transfer.

Open quantum systems have their internal energy levels shifted when they interact with an environment - the so-called Lamb shift, which takes place in a wide range of systems [11]. The shift can even become time-dependent if the environment fluctuates temporally, *e.g.* the AC Stark effect, where oscillating electric fields cause a temporal shift in energy [12]. An example relevant to this work is that of a strongly coupled system of an exciton and a phonon. Here, the transfer of the exciton between dipole-interacting molecules causes the phonon to be in a nonequilibrium state, which leads to fluctuations in the energy levels of the molecules supporting the excitonic transfer. In this Letter, we investigate a time-dependent Lamb shift induced by phonon modes that are shared by the interacting molecules, causing the energy-level fluctuations of the molecules to become highly correlated. We consider the non-adiabatic regime where the frequency of the phonons ω is comparable in magnitude to the dipole coupling J between the molecules. We find that the resonance conditions for the exciton transfer are dynamically satisfied as a direct consequence of this time-dependent Lamb shift due to phonon dynamics. This leads to interesting energy transport features: (a) Excitonic hopping between molecules is dynamically conditioned (dynamic resonance), (b) The exciton transfer can be biased toward a particular direction (directionality), and (c) The exciton moves rapidly by interfering with itself (quantum walk). We show that this mechanism, which we call phonon-induced dynamic resonance energy transfer (DRET), enables long-range energy transport combined with quantum speed-up, even in the presence of considerable disorder in molecular energies. Our work shows that sharing phonons between neighboring molecules not only protects quantum

coherence [8, 9], similar in spirit to decoherence-free subspaces [13], but also enables the harnessing of quantum coherence for long-range energy transport in highly disordered systems. Our results highlight some exciting possibilities for future hybrid quantum phononic systems, with the features of the described mechanism having the potential to open up new functionalities for designing quantum transport devices and networks.

Resonance and disorder.—In both classical and quantum energy transport systems, resonance plays a vital role. In classical transport, with a phonon environment present, resonant incoherent energy transfer occurs for a downhill energy gradient, a mechanism well known as Förster resonance energy transfer (FRET) [4]. Once an exciton hops incoherently from a high to a low energy molecule, the energy difference is dissipated by phonon relaxation, leading to funneling of the exciton through the molecules. However, in the presence of local energetic traps, due to disorder in the energy levels of the molecules, downhill diffusion leads to trapping of the exciton at the energetic minima, suppressing long-range energy transport. In quantum transport, on the other hand, resonant coherent energy transfer from a donor to an acceptor molecule occurs in the absence of energy-level mismatches, as shown in Fig. 1(a). In the presence of disorder the transfer then becomes non-resonant and again long-range energy transport is suppressed.

Exciton and shared phonon.—We now show that when different molecules are coupled to the same phonon, the necessary resonance conditions for quantum transport can be satisfied by the dynamics of the phonon, even in the presence of significant disorder in molecular energies. Consider the case where phonon relaxation is absent and the total energy of an excitonic polaron system is conserved. For a chain of N molecules, the Hamiltonian of the system in the single-exciton manifold is

$$\hat{H} = \sum_{j=1}^N \hat{E}_j(\hat{p}, \hat{q}) |j\rangle \langle j| + \sum_{j \neq k} \hbar J_{jk} |j\rangle \langle k|, \quad (1)$$

with $|j\rangle$ a single-exciton state where molecule j is excited and all other molecules are in their ground states, $\hat{E}_j(\hat{p}, \hat{q})$ is the excitonic polaron energy operator and $\hbar J_{jk}$ is the dipolar coupling responsible for exciton hopping. The operator $\hat{E}_j(\hat{p}, \hat{q})$ is given by

$$\hat{E}_j(\hat{p}, \hat{q}) = \hbar\Omega_j + \frac{\hat{p}^2}{2m} + \frac{1}{2}m\omega^2(\hat{q} - d_j)^2, \quad (2)$$

where $\hbar\Omega_j$ is the excited energy of molecule j and ω is the frequency of the phonon mode associated with position \hat{q} and momentum \hat{p} . The equilibrium position d_j of the phonon mode is assumed to be deformed by the molecular excitation. Using the creation and annihilation operators of the phonon, \hat{b}^\dagger and \hat{b} , the Hamiltonian can be decomposed as $\hat{H} = \hat{H}_e + \hat{H}_{\text{ph}} + \hat{H}_{e-\text{ph}}$. The first term describes the electronic states of the molecules $\hat{H}_e = \sum_{j=1}^N \hbar(\Omega_j + f_j^2 \omega^{-1}) |j\rangle \langle j| + \sum_{j \neq k} \hbar J_{jk} |j\rangle \langle k|$, the second term describes the phonon $\hat{H}_{\text{ph}} = \hbar\omega(\hat{b}^\dagger \hat{b} + \frac{1}{2})$, and the last term describes the interaction between exciton and phonon $\hat{H}_{e-\text{ph}} = -\sum_{j=1}^N \hbar f_j |j\rangle \langle j| \otimes (\hat{b}^\dagger + \hat{b})$, with $f_j =$

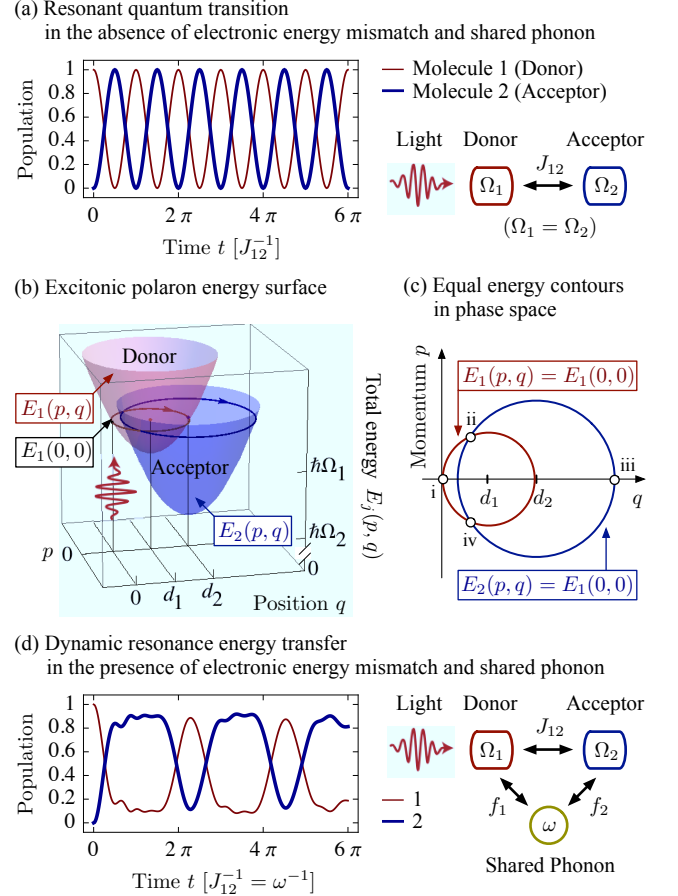


FIG. 1: (Color online) A two-molecule system with initial state $|I\rangle = |1\rangle$. In (a), where $(\Omega_1 - \Omega_2)/J_{12} = 0$ and $f_1 = f_2 = 0$, resonant exciton hopping mediated by a dipolar coupling J_{12} occurs and oscillates in time. In (b)-(d), where $\omega/J_{12} = 1$, $(\Omega_1 - \Omega_2)/J_{12} = 2$, $f_1/J_{12} = 1$ and $f_2/J_{12} = 2$, a shared phonon in a nonequilibrium state leads to dynamic resonance energy transfer. A quantum picture of the phonon dynamics in phase space can be represented using the Wigner function [15] (a video is included in the Supplemental Material).

$\sqrt{m\omega^3(2\hbar)^{-1}}d_j$, leading to fluctuations of the molecule energy levels. We assume that the total system is initially in the state $|I\rangle \otimes |0\rangle_{\text{ph}}$ at time $t = 0$, where $|I\rangle$ is the initial single-exciton state and $|0\rangle_{\text{ph}}$ is the ground state of the phonon defined by $\hat{H}_{\text{ph}} |0\rangle_{\text{ph}} = \frac{1}{2}\hbar\omega |0\rangle_{\text{ph}}$. The time evolution of the total system is $\sum_{k=1}^N |k\rangle \otimes |\psi_k(t)\rangle$, with $P_k(t) = \langle \psi_k(t) | \psi_k(t) \rangle$ representing the population of molecule k at time t .

Dynamic resonance.—To clarify the principle of DRET, we start with a two-molecule system. Here, once a donor is excited (molecule 1), the phonon mode has its equilibrium position displaced by d_1 , due to a deformation in the structural support of the system. Then the phonon is in a nonequilibrium state, moving along an equal energy contour $E_1(p, q) = E_1(0, 0)$ in phase space of momentum p and position q , as shown in Figs. 1(b) and (c). Here, $E_1(p, q)$ is the energy of the total system including the electronic energy of the donor $\hbar\Omega_1$ and the phonon energy. $E_1(0, 0)$ is the initial energy of the total system. During the phonon's dynamics, if the equilibrium position of the phonon mode depends

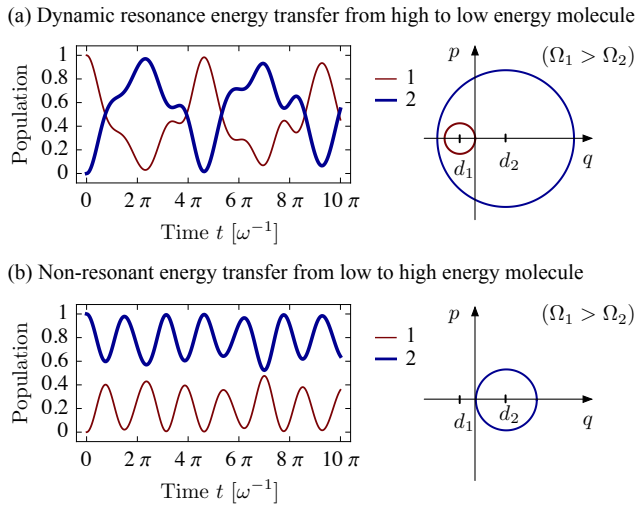


FIG. 2: (Color online) Once an exciton is created at molecule j , the equal energy contours $E_k(p, q) = E_j(0, 0)$ are determined in phase space. If the contours are close enough such that the total energy difference is small compared to the dipolar coupling, $|E_1(p, q) - E_2(p, q)| < \hbar J_{12}$, near-resonant exciton transfer takes place. If not, the exciton transfer is suppressed by non-resonance. Here we take $\omega/J_{12} = 2.4$, $(\Omega_1 - \Omega_2)/J_{12} = 2$, $f_1/J_{12} = -0.5$ and $f_2/J_{12} = 1$. In (a), where $|I\rangle = |1\rangle$, an exciton created at molecule 1 is transferred from a high to a low energy molecule by dynamic resonance. In (b), where $|I\rangle = |2\rangle$, an exciton created at molecule 2 is localized at the low energy molecule 2 by non-resonance.

on the state of the molecules due to a different deformation in the structural support, *i.e.* $d_1 \neq d_2$, the energy level of an acceptor (molecule 2) $E_2(p, q)$ will oscillate in time [16]. While the phonon moves along contour $E_1(p, q) = E_1(0, 0)$, when the energy level of the acceptor becomes equal to that of the donor, $E_1(p, q) = E_2(p, q)$, there is a high probability for resonant exciton hopping from the donor to the acceptor to take place with the conservation of energy and momentum of the total system. This happens at an intersection (point (ii) in Fig. 1(c)) between different energy contours $E_1(p, q) = E_1(0, 0)$ and $E_2(p, q) = E_1(0, 0)$. When the acceptor becomes excited, the phonon moves along contour $E_2(p, q) = E_1(0, 0)$. This leads to temporal oscillations in the energy level of the donor $E_1(p, q)$ and non-resonance of the exciton transfer until the phonon arrives at another intersection (point (iv)). This phonon-induced dynamic resonance energy transfer (DRET) takes place even in the presence of electronic energy mismatches $\Omega_1 \neq \Omega_2$. In the presence of the mismatch, the radii of equal energy contours are different, as shown in Fig. 1(c), which leads to an asymmetry in the time evolution of the populations of the molecules, such that the exciton stays at the lower energy molecule 2 for longer, as shown in Fig. 1(d). Here the energy of the excitonic polaron is partially transferred from the exciton to the phonon and back again without dissipation in order to allow the transfer to take place. This reversible exchange of energy enables efficient energy transfer even in rugged electronic energy landscapes with energetic traps, as shown in Fig. S1 of the Supplemental Material.

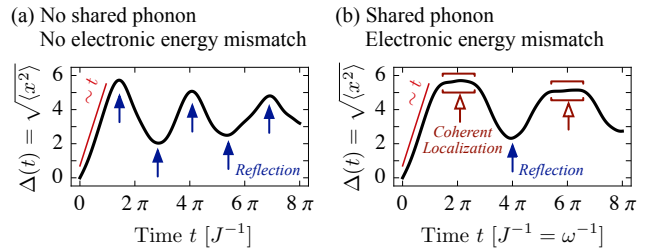


FIG. 3: (Color online) A seven-molecule linear chain with $|I\rangle = |1\rangle$, $J_{jk} = J$ if $j = k \pm 1$ and $J_{jk} = 0$ otherwise. The distance between neighboring molecules is assumed to be uniform such that $\Delta(t) = \sqrt{\langle x^2 \rangle} = (\sum_{k=1}^7 (k-1)^2 P_k(t))^{1/2}$. In (a), we take $\Omega_j = \Omega_k$ and $f_j = 0$ for all j and k , which leads to a quantum walk in a chain of finite size where an exciton is transferred back and forth through the molecules with quantum speed-up due to the reflection at the boundaries of the chain. In (b), the chain is coupled to a shared phonon mode with nonzero f_j . Even in the presence of electronic energy mismatches, an exciton can be transferred with quantum speed-up by dynamic resonance. When molecule 7, located at one of the boundaries, has the lowest electronic energy, the exciton is temporally trapped at the molecule due to the non-resonance induced by the phonon dynamics. The Supplemental Material provides the values of the parameters used and the time evolution of the populations of the molecules (cf. Fig. S5).

Directionality.—Remarkably, DRET can also induce directionality, similar to a diode in electrical circuitry. In direct contrast to FRET, where the energy transfer is always biased toward a lower energy molecule, DRET can induce directionality in both downhill and uphill directions, such that the transfer becomes biased from a high to a low energy molecule $\Omega_1 > \Omega_2$, as shown in Fig. 2, or from a low to a high energy molecule $\Omega_1 < \Omega_2$, as shown in Fig. S3. This directionality is induced by the resonance of the transition, such that energy transfer in a particular direction is enhanced by dynamic resonance, while in the opposite direction it is suppressed by non-resonance. Directionality can also be induced in a chain of molecules, as shown in Fig. S4.

Quantum walk.—In a large chain, DRET also enables long-range energy transport that is otherwise unavailable. In the absence of energy mismatches, a coherent exciton moves very quickly by interfering with itself similar to a quantum walk. Here the root mean square displacement $\Delta(t) = \sqrt{\langle x^2 \rangle}$ increases linearly with time t , $\Delta(t) \propto t$, where x is the distance that the exciton moves during time t [2]. In the presence of energy mismatches, however, quantum coherence leads to coherent localization of the exciton, similar to Anderson localization [14]. A new and rather surprising feature introduced by DRET is that when electronic energy mismatches are present and a shared phonon is available, both quantum walk and coherent localization can occur concurrently, where an exciton moves through a chain with quantum speed-up and is subsequently localized at a particular molecule for a period without losing quantum coherence, as shown in Fig. 3.

Phonon relaxation and thermal noise.—So far only a single shared phonon mode has been considered. As the number of shared phonon modes is increased leading to a shared bath, phonon relaxation takes place, suppressing the reversibility of

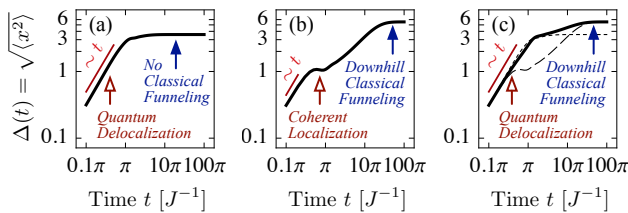


FIG. 4: (Color online) A seven-molecule linear chain with $J_{jk} = J$ if $j = k \pm 1$ and $J_{jk} = 0$ otherwise. In each panel, when an exciton is created at molecule 1, it is transferred through the molecules, while thermal noise of the phonon bath at temperature T destroys quantum coherence, leading to a quantum-to-classical transition in the exciton transfer. Here, as an example, we take environment couplings such that quantum transport takes place up to $t \approx \pi J^{-1}$ and classical transport occurs subsequently (cf. Fig. S6). (a) In the presence of local baths, when all the molecules have the same electronic energy, long-range quantum delocalization takes place due to resonance, but no classical funneling occurs due to the absence of a downhill energy gradient, $\Delta(t \rightarrow 100\pi) = \sqrt{\langle x^2 \rangle} \approx (\sum_{k=1}^7 (k-1)^2 \frac{1}{7})^{1/2} \approx 3.6$. (b) On the other hand, when the energy gradient is comparable to, or larger in magnitude than the thermal energy $k_B T$, downhill classical funneling takes place, but non-resonance induces coherent localization, leading to short-range quantum delocalization. (c) In the presence of a shared phonon bath, however, a time-dependent Lamb shift takes place such that a near-flat energy landscape evolves into a downhill landscape via phonon relaxation. In this case, long-range quantum delocalization and subsequent classical funneling can be utilized for enhancing the overall exciton transfer: in (c), the dotted and dashed lines display $\Delta(t)$ in (a) and (b) for comparison. The Supplemental Material provides a non-Markovian quantum master equation and the values of the parameters used.

DRET. Here, once an exciton hops from a high to low energy molecule by dynamic resonance, it is trapped at the lower energy molecule due to phonon relaxation, enhancing the directionality of the exciton transfer. On the other hand, in the presence of thermal noise, DRET is degraded as quantum coherent effects are suppressed by decoherence and the trapped exciton at the lower energy molecule may be released by absorbing thermal energy. Despite the detrimental effects of phonon relaxation and thermal noise, DRET can enhance exciton transfer in disordered systems by exploiting an interplay between quantum delocalization and classical funneling, as shown in Fig. 4. This suggests that sharing phonons between molecules not only enhances the coherent timescale of exciton transfer, as shown in previous studies [8, 9], but also enables the utilizing of quantum coherence for efficient energy transport in disordered systems.

Summary.—We investigated a shared phonon in the nonequilibrium regime and its influence on the exciton transfer in a chain of molecules. We showed that the time-dependent Lamb shift induced by phonon dynamics leads to interesting energy transport features, such as dynamic resonance, directionality and quantum walk. This work opens up some intriguing possibilities for quantum transport in disordered systems in general. Contrary to the widely accepted notion that quantum coherence is not useful for energy transport in disordered systems, our results show that phonons can enable a quantum speed-up in energy transport, regardless

of significant disorder. The consideration of more complex shared phonon dynamics may lead to new transport mechanisms like DRET being discovered, providing features that are unavailable in systems investigated so far. Thus, we expect our findings to unlock the engineering of novel quantum transport schemes in disordered nanostructures.

We are grateful to M. S. Kim and M. B. Plenio for useful comments. This work was supported by National Research Foundation of Korea grants funded by the Korean Government (Ministry of Education, Science and Technology; grant numbers 2010-0018295 and 2010-0015059), the UK's Engineering and Physical Sciences Research Council, and the Leverhulme Trust.

* Electronic address: m.tame@imperial.ac.uk

† Electronic address: hyoung@hanyang.ac.kr

- [1] M. A. Nielsen and I. L. Chuang, *Quantum Computation and Quantum Information* (Cambridge University Press, Cambridge, 2000).
- [2] Y. Aharonov, L. Davidovich, and N. Zagury, *Phys. Rev. A* **48**, 1687 (1993).
- [3] D. Braun, *Phys. Rev. Lett.* **89**, 277901 (2002); M. S. Kim, J. Lee, D. Ahn, and P. L. Knight, *Phys. Rev. A* **65**, 040101(R) (2002).
- [4] T. Förster, *Ann. Phys.* **437**, 55 (1948).
- [5] T. F. Soules and C. B. Duke, *Phys. Rev. B* **3**, 262 (1971).
- [6] J. D. Teufel, T. Donner, D. Li, J. W. Harlow, M. S. Allman, K. Cicak, A. J. Sirois, J. D. Whittaker, K. W. Lehnert, and R. W. Simmonds, *Nature* **475**, 359 (2011); J. Chan, T. P. M. Alegre, A. H. Safavi-Naeini, J. T. Hill, A. Krause, S. Gröblacher, M. Aspelmeyer, and O. Painter, *Nature* **478**, 89 (2011); M. Eichenfield, J. Chan, R. M. Camacho, K. J. Vahala, and O. Painter, *Nature* **462**, 78 (2009); A. D. O'Connell, M. Hofheinz, M. Ansmann, R. C. Bialczak, M. Lenander, E. Lucero, M. Neeley, D. Sank, H. Wang, M. Weides, J. Wenner, J. M. Martinis, and A. N. Cleland, *Nature* **464**, 697 (2010).
- [7] H. Lee, Y.-C. Cheng, and G. R. Fleming, *Science* **316**, 1462 (2007); J. R. Caram, N. H. C. Lewis, A. F. Fidler, and G. S. Engel, *J. Chem. Phys.* **136**, 104505 (2012); A. Kolloi, E. J. O'Reilly, G. D. Scholes, and A. Olaya-Castro, *J. Chem. Phys.* **137**, 174109 (2012); A. W. Chin, S. F. Huelga and M. B. Plenio, *Phil. Trans. R. Soc. A* **370**, 3638 (2012); A. W. Chin, J. Prior, R. Rosenbach, F. Caycedo-Soler, S. F. Huelga and M. B. Plenio, *Nature Phys.* **9**, 113 (2013).
- [8] A. Nazir, *Phys. Rev. Lett.* **103**, 146404 (2009); D. P. S. McCutcheon and A. Nazir, *Phys. Rev. B* **83**, 165101 (2011).
- [9] J. Wu, F. Liu, Y. Shen, J. Cao, and R. J. Silbey, *New J. Phys.* **12**, 105012 (2010); A. Ishizaki and G. R. Fleming, *New J. Phys.* **12**, 055004 (2010); H. Hossein-Nejad and G. D. Scholes, *New J. Phys.* **12**, 065045 (2010); P. Nalbach, J. Eckel, and M. Thorwart, *New J. Phys.* **12**, 065043 (2010).
- [10] B. Wolfseider and W. Domcke, *Chem. Phys. Lett.* **259**, 113 (1996).
- [11] H.-P. Breuer and F. Petruccione, *The Theory of Open Quantum Systems* (Oxford University Press, Oxford, 2002).
- [12] S. H. Autler and C. H. Townes, *Phys. Rev.* **100**, 703 (1955).
- [13] D. A. Lidar, I. L. Chuang, and K. B. Whaley, *Phys. Rev. Lett.* **81**, 2594 (1998).
- [14] P. W. Anderson, *Phys. Rev.* **109**, 1492 (1958).
- [15] E. Wigner, *Phys. Rev.* **40**, 749 (1932).
- [16] The energy-level mismatch between molecules 1 and 2 is given by $E_1(p, q) - E_2(p, q) = -m\omega^2(d_1 - d_2)q + \hbar(\Omega_1 - \Omega_2) + \frac{1}{2}m\omega^2(d_1^2 - d_2^2)$, which depends on the time evolution of q when $d_1 \neq d_2$.

SUPPLEMENTARY INFORMATION

In section I, we provide the theoretical model of the shared phonon bath used in Figs. 4 and S6. In section II, we provide values for the parameters used in all simulations.

SECTION I. THEORETICAL MODEL OF SHARED PHONON BATH

Hamiltonian

We consider a molecular chain coupled to a shared phonon bath modeled by a set of quantum harmonic oscillators. The Hamiltonian in the single-exciton manifold consists of three parts $\hat{H} = \hat{H}_e + \hat{H}_{\text{ph}} + \hat{H}_{e-\text{ph}}$. The first term describes the electronic states of the molecules

$$\hat{H}_e = \sum_{j=1}^N \hbar(\Omega_j + \lambda_j(1 + 2s_j)) |j\rangle \langle j| + \sum_{j \neq k} \hbar J_{jk} |j\rangle \langle k|, \quad (1)$$

where $\lambda_j = \sum_{\xi} g_{j\xi}^2 \omega_{\xi}^{-1}$, $\lambda_j(1 + 2s_j)$ is the Lamb shift induced by the interaction between molecule j and the phonons. The second term describes the phonons $\hat{H}_{\text{ph}} = \sum_{\xi} \hbar \omega_{\xi} \hat{b}_{\xi}^{\dagger} \hat{b}_{\xi}$, where \hat{b}_{ξ}^{\dagger} and \hat{b}_{ξ} are creation and annihilation operators of a phonon mode ξ with frequency ω_{ξ} . The last term describes the interaction between the molecules and phonons

$$\hat{H}_{e-\text{ph}} = - \sum_{j=1}^N \sum_{\xi} \hbar g_{j\xi} (|j\rangle \langle j| + s_j \sum_{k=1}^N |k\rangle \langle k|) \otimes (\hat{b}_{\xi}^{\dagger} + \hat{b}_{\xi}). \quad (2)$$

When $s_j = 0$ for all j , $\hat{H}_{e-\text{ph}}$ describes local phonon baths: for a phonon mode ξ coupled to molecule j by $g_{j\xi} \neq 0$, we assume $g_{k\xi} = 0$ for all $k \neq j$. For nonzero s_j , $\hat{H}_{e-\text{ph}}$ describes a shared phonon bath where each phonon mode ξ is coupled to all the molecules by $g_{j\xi}s_j$, except for molecule j which is coupled by $g_{j\xi}(1 + s_j)$. The difference in $g_{j\xi}$ leads to decoherence of the electronic coherence, while $g_{j\xi}s_j$ induces a time-dependent Lamb shift without additional decoherence, as shown below.

The dynamics of the exciton transfer are described by the reduced electronic state $\hat{\rho}_e(t) = \text{Tr}_{\text{ph}}[\hat{\rho}(t)]$, where $\hat{\rho}(t)$ is the total state and Tr_{ph} is the partial trace over phonons. We take the state of the total system at time $t = 0$ to be $\hat{\rho}(0) = \hat{\rho}_e(0) \otimes Z^{-1} \exp(-\beta \hat{H}_{\text{ph}})$, where $\hat{\rho}_e(0)$ is the initial single-exciton state and $Z^{-1} \exp(-\beta \hat{H}_{\text{ph}})$ is a thermal state at temperature $T = (k_B \beta)^{-1}$, with $Z = \text{Tr}_{\text{ph}}[\exp(-\beta \hat{H}_{\text{ph}})]$.

Derivation of time-dependent Lamb shift

Here we derive an effective Hamiltonian $\hat{H}^{\text{eff}}(t)$ that gives exactly the same exciton transfer dynamics, described by the state $\hat{\rho}_e(t)$, as obtained by the original Hamiltonian \hat{H} ,

$$\hat{\rho}_e(t) = \text{Tr}_{\text{ph}}[\exp(-\frac{i}{\hbar} \hat{H} t) \hat{\rho}(0) \exp(\frac{i}{\hbar} \hat{H}^{\dagger} t)] = \text{Tr}_{\text{ph}} \left[\mathcal{T} \exp\left(-\frac{i}{\hbar} \int_0^t \hat{H}^{\text{eff}}(t') dt'\right) \hat{\rho}(0) \mathcal{T}^{\dagger} \exp\left(\frac{i}{\hbar} \int_0^t \hat{H}^{\text{eff}\dagger}(t') dt'\right) \right], \quad (3)$$

where \mathcal{T} and \mathcal{T}^{\dagger} denote the chronological and anti-chronological time ordering operators. The effective Hamiltonian consists of three parts $\hat{H}^{\text{eff}}(t) = \hat{H}_e^{\text{eff}}(t) + \hat{H}_{\text{ph}} + \hat{H}_{e-\text{ph}}^{\text{eff}}$, where $\hat{H}_e^{\text{eff}}(t)$ is an effective Hamiltonian of the electronic states of the molecules including time-dependent Lamb shift

$$\hat{H}_e^{\text{eff}}(t) = \sum_{j=1}^N \hbar(\Omega_j + \lambda_j + 2s_j \sum_{\xi} g_{j\xi}^2 \omega_{\xi}^{-1} \cos(\omega_{\xi} t)) |j\rangle \langle j| + \sum_{j \neq k} \hbar J_{jk} |j\rangle \langle k|, \quad (4)$$

and $\hat{H}_{e-\text{ph}}^{\text{eff}}$ is an effective Hamiltonian describing decoherence of the electronic coherence

$$\hat{H}_{e-\text{ph}}^{\text{eff}} = \sum_{j=1}^N \sum_{\xi} \hbar g_{j\xi} |j\rangle \langle j| \otimes (\hat{b}_{\xi}^{\dagger} + \hat{b}_{\xi}). \quad (5)$$

The effective Hamiltonian provides the analytic form of the time-dependent Lamb shift induced by shared phonon dynamics, *i.e.* $2\hbar s_j \sum_{\xi} g_{j\xi}^2 \omega_{\xi}^{-1} \cos(\omega_{\xi} t)$. It also enables one to employ well-developed non-Markovian approaches [1, 2], which have been developed to describe the interaction between molecules and phonons in the form of Eq. (5), as shown below. We derive the

effective Hamiltonian $\hat{H}_e^{\text{eff}}(t)$ and the time-dependent Lamb shift of $\hat{H}_e^{\text{eff}}(t)$ with the use of a path integral representation of the reduced electronic state $\hat{\rho}_e(t)$ and an influence functional developed by Feynman and Vernon [3].

To implement a path integral representation, we start with the formal expression of the reduced electronic state of molecules $\hat{\rho}_e(t)$

$$\hat{\rho}_e(t) = \text{Tr}_{\text{ph}} \left[\exp\left(-\frac{i}{\hbar} \hat{H} t\right) \hat{\rho}(0) \exp\left(\frac{i}{\hbar} \hat{H}^\dagger t\right) \right]. \quad (6)$$

By splitting the time t into M divisions, *i.e.* $t = M\Delta t$, the single-exciton state at time t can be expressed as

$$\hat{\rho}_e(t) = \text{Tr}_{\text{ph}} \left[\exp\left(-\frac{i}{\hbar} \hat{H} M\Delta t\right) \hat{\rho}(0) \exp\left(\frac{i}{\hbar} \hat{H}^\dagger M\Delta t\right) \right] \quad (7)$$

$$= \text{Tr}_{\text{ph}} \left[\exp\left(-\frac{i}{\hbar} \hat{H} \Delta t\right) \times \cdots \times \exp\left(-\frac{i}{\hbar} \hat{H} \Delta t\right) \hat{\rho}(0) \exp\left(\frac{i}{\hbar} \hat{H}^\dagger \Delta t\right) \times \cdots \times \exp\left(\frac{i}{\hbar} \hat{H}^\dagger \Delta t\right) \right]. \quad (8)$$

We then substitute an identity operator $\mathbb{1} = \sum_{k=1}^N |k\rangle \langle k|$ of the single-exciton subspace at the front and back of each time evolution operator $\exp(-i\hat{H}\Delta t/\hbar)$ or $\exp(i\hat{H}^\dagger\Delta t/\hbar)$ for a time increment Δt

$$\hat{\rho}_e(t) = \text{Tr}_{\text{ph}} \left[\mathbb{1} \exp\left(-\frac{i}{\hbar} \hat{H} \Delta t\right) \mathbb{1} \times \cdots \times \mathbb{1} \exp\left(-\frac{i}{\hbar} \hat{H} \Delta t\right) \mathbb{1} \hat{\rho}(0) \mathbb{1} \exp\left(\frac{i}{\hbar} \hat{H}^\dagger \Delta t\right) \mathbb{1} \times \cdots \times \mathbb{1} \exp\left(\frac{i}{\hbar} \hat{H}^\dagger \Delta t\right) \mathbb{1} \right] \quad (9)$$

$$= \sum_{k_M^+=1}^N \sum_{k_M^- =1}^N |k_M^+\rangle \langle k_M^-| \sum_{k_0^+=1}^N \sum_{k_0^- =1}^N \cdots \sum_{k_{M-1}^+=1}^N \sum_{k_{M-1}^- =1}^N \times \text{Tr}_{\text{ph}} \left[\left(\prod_{l=0}^{M-1} \langle k_{l+1}^+ | \exp\left(-\frac{i}{\hbar} \hat{H} \Delta t\right) | k_l^+ \rangle \right) \langle k_0^+ | \hat{\rho}(0) | k_0^- \rangle \left(\prod_{l=0}^{M-1} \langle k_l^- | \exp\left(\frac{i}{\hbar} \hat{H}^\dagger \Delta t\right) | k_{l+1}^- \rangle \right) \right], \quad (10)$$

where the superscripts \pm and subscripts l of the k_l^\pm with non-negative integers $l \in \{0, 1, \dots, M\}$ are introduced to distinguish identity operators in different positions. The partial trace over phonon degrees of freedom Tr_{ph} in Eq. (10) can be carried out with the use of an influence functional [3]. The reduced electronic state is then expressed as

$$\hat{\rho}_e(t) = \sum_{k_M^+=1}^N \sum_{k_M^- =1}^N |k_M^+\rangle \langle k_M^-| \sum_{k_0^+=1}^N \sum_{k_0^- =1}^N \cdots \sum_{k_{M-1}^+=1}^N \sum_{k_{M-1}^- =1}^N \mathcal{I}(k_0^+, k_0^-, \dots, k_M^+, k_M^-) \times \left(\prod_{l=0}^{M-1} \langle k_{l+1}^+ | \exp\left(-\frac{i}{\hbar} \hat{H}_e \Delta t\right) | k_l^+ \rangle \right) \langle k_0^+ | \hat{\rho}_e(0) | k_0^- \rangle \left(\prod_{l=0}^{M-1} \langle k_l^- | \exp\left(\frac{i}{\hbar} \hat{H}_e^\dagger \Delta t\right) | k_{l+1}^- \rangle \right), \quad (11)$$

where $\mathcal{I}(k_0^+, k_0^-, \dots, k_M^+, k_M^-)$ is the so-called influence functional that is responsible for the influence of the phonon bath on the electronic system dynamics. In the continuous limit, *i.e.* $\Delta t \rightarrow 0$ or equivalently $M \rightarrow \infty$, the influence functional $\mathcal{I} = \lim_{\Delta t \rightarrow 0} \mathcal{I}(k_0^+, k_0^-, \dots, k_M^+, k_M^-)$ can be decomposed into two parts

$$\mathcal{I} = \mathcal{I}_D \times \mathcal{I}_{\text{LS}}, \quad (12)$$

where the first term \mathcal{I}_D is responsible for environmental decoherence of the electronic coherence

$$\mathcal{I}_D = \prod_{j=1}^N \exp \left\{ - \int_0^t dt' \int_0^{t'} dt'' [\delta(j, k^+(t')) - \delta(j, k^-(t'))] [\alpha_j(t' - t'') \delta(j, k^+(t'')) - \alpha_j^*(t' - t'') \delta(j, k^-(t''))] \right\}, \quad (13)$$

and the second term \mathcal{I}_{LS} is responsible for dynamic resonance

$$\mathcal{I}_{\text{LS}} = \prod_{j=1}^N \exp \left\{ -i \int_0^t dt' [\delta(j, k^+(t')) - \delta(j, k^-(t'))] 2s_j \left[\sum_{\xi} g_{j\xi}^2 \omega_{\xi}^{-1} \cos(\omega_{\xi} t') - \lambda_j \right] \right\}, \quad (14)$$

with $\lambda_j = \sum_{\xi} g_{j\xi}^2 \omega_{\xi}^{-1}$, leading to a time-dependent Lamb shift $2\hbar s_j \left[\sum_{\xi} g_{j\xi}^2 \omega_{\xi}^{-1} \cos(\omega_{\xi} t') - \lambda_j \right]$. Note that the subscript l of k_l^\pm for a finite time increment Δt is replaced with a continuous variable t' or t'' such that $k_l^\pm \rightarrow k^\pm(t_l)$ with $t_l = l\Delta t$ as $\Delta t \rightarrow 0$. Here, $\delta(j, k)$ is the Kronecker delta defined by $\delta(j, k) = 1$ if $j = k$ and $\delta(j, k) = 0$ otherwise, and $\alpha_j(\tau)$ is a bath response function characterized by the spectral density $\Lambda_j(\omega) = \sum_{\xi} \hbar g_{j\xi}^2 \delta(\omega - \omega_{\xi})$

$$\alpha_j(\tau) = \sum_{\xi} g_{j\xi}^2 \left[\coth\left(\frac{\hbar\omega_{\xi}\beta}{2}\right) \cos(\omega_{\xi}\tau) - i \sin(\omega_{\xi}\tau) \right] \quad (15)$$

$$= \frac{1}{\hbar} \int_0^{\infty} d\omega \Lambda_j(\omega) \left[\coth\left(\frac{\hbar\omega\beta}{2}\right) \cos(\omega\tau) - i \sin(\omega\tau) \right]. \quad (16)$$

Hence, in the continuous limit $\Delta t \rightarrow 0$, the reduced electronic state can be expressed as

$$\begin{aligned} \hat{\rho}_e(t) = & \sum_{k_M^+=1}^N \sum_{k_M^-=1}^N |k_M^+\rangle \langle k_M^-| \sum_{k_0^+=1}^N \sum_{k_0^-=1}^N \cdots \sum_{k_{M-1}^+=1}^N \sum_{k_{M-1}^-=1}^N \mathcal{I}_D(k_0^+, k_0^-, \dots, k_M^+, k_M^-) \\ & \times \left(\prod_{l=0}^{M-1} \langle k_{l+1}^+ | \exp(-\frac{i}{\hbar} \hat{H}_e^{\text{eff}}(t_l) \Delta t) | k_l^+ \rangle \right) \langle k_0^+ | \hat{\rho}_e(0) | k_0^- \rangle \left(\prod_{l=0}^{M-1} \langle k_l^- | \exp(\frac{i}{\hbar} \hat{H}_e^{\text{eff}\dagger}(t_l) \Delta t) | k_{l+1}^- \rangle \right), \end{aligned} \quad (17)$$

with $t_l = l\Delta t$, $\hat{H}_e^{\text{eff}}(t)$ is the effective Hamiltonian of the electronic states of the molecules including time-dependent Lamb shift in Eq. (4). This implies that the effective Hamiltonian $\hat{H}_e^{\text{eff}}(t)$ gives exactly the same exciton transfer dynamics $\hat{\rho}_e(t)$ as obtained by the original total Hamiltonian \hat{H} . For an arbitrary form of the spectral densities $\Lambda_j(\omega)$, the dynamics of the reduced electronic state $\hat{\rho}_e(t)$ can be calculated using a path-integral approach, known as the iterative real-time quasiadiabatic propagator path-integral (QUAPI) scheme [1]. In this work, however, we take an Ohmic spectral density with a Lorentz-Drude cutoff function $\Lambda_j(\omega) = \sum_{\xi} \hbar g_{j\xi}^2 \delta(\omega - \omega_{\xi}) = (2\hbar\lambda_j/\pi)\omega\gamma_j/(\omega^2 + \gamma_j^2)$ with the phonon relaxation rate γ_j to employ the so-called hierarchical approach, which is a computationally efficient framework to simulate exciton transfer dynamics [2]. The time-dependent Lamb shift then becomes $2\hbar s_j \sum_{\xi} g_{j\xi}^2 \omega_{\xi}^{-1} \cos(\omega_{\xi} t) = 2\hbar s_j \lambda_j e^{-\gamma_j t}$. This implies that the shared phonon bath induces dynamic resonance such that the effective energy landscape that an exciton feels during transport changes in time $\hbar\Omega_j + \hbar\lambda_j(1 + 2s_j e^{-\gamma_j t})$.

Hierarchically coupled master equations in the presence of a shared phonon bath

Here we provide a non-Markovian quantum master equation, represented by a collection of hierarchically coupled master equations, that reliably describes exciton transfer dynamics in the presence of a shared phonon bath.

With the shared phonon bath modeled by the Ohmic spectral density and the high temperature condition characterized by $\beta\hbar\gamma_j < 1$ taken [2], the time evolution of the reduced electronic state $\hat{\rho}_e(t)$ can be modeled by the following hierarchically coupled master equations

$$\frac{d}{dt} \hat{\sigma}(\vec{n}, t) = -\frac{i}{\hbar} \left[\hat{H}_e^{\text{eff}}(t), \hat{\sigma}(\vec{n}, t) \right] - \sum_{j=1}^N n_j \gamma_j \hat{\sigma}(\vec{n}, t) + \sum_{j=1}^N \hat{\Phi}_j[\hat{\sigma}(\vec{n}_{j+}, t)] + \sum_{j=1}^N n_j \hat{\Theta}_j[\hat{\sigma}(\vec{n}_{j-}, t)], \quad (18)$$

where $\hat{H}_e^{\text{eff}}(t)$ is the effective Hamiltonian of the electronic states in Eq. (4) and $\vec{n} = \{n_1, \dots, n_N\}$ with non-negative integers $n_j \in \{0, 1, \dots\}$. The vectors $\vec{n}_{j\pm}$ differ from \vec{n} only by changing n_j to $n_j \pm 1$, *i.e.* $\vec{n}_{j\pm} = \{n_1, \dots, n_j \pm 1, \dots, n_N\}$. In the above, the reduced electronic state is the lowest rank operator $\hat{\rho}_e(t) = \hat{\sigma}(\vec{0}, t)$ with $\vec{0} = \{0, \dots, 0\}$. The other auxiliary operators $\hat{\sigma}(\vec{n}, t)$ are introduced in order to take into account environmental decoherence of electronic coherence. Their dimensions are the same as that of the reduced electronic state $\hat{\rho}_e(t)$. At initial time $t = 0$, just after an exciton is created in a molecular chain, $\hat{\sigma}(\vec{0}, 0) = \hat{\rho}_e(0)$ and all the other auxiliary operators are set to be zero, *i.e.* $\hat{\sigma}(\vec{n}, 0) = 0$ for all $\vec{n} \neq \vec{0}$. The last two terms in the coupled master equations produce a coupling between the operators of different ranks $N_{\text{rank}} = \sum_{j=1}^N n_j$, which are given by

$$\hat{\Phi}_j[\hat{\sigma}(\vec{n}_{j+}, t)] = i[|j\rangle \langle j|, \hat{\sigma}(\vec{n}_{j+}, t)], \quad (19)$$

$$\hat{\Theta}_j[\hat{\sigma}(\vec{n}_{j-}, t)] = i \frac{2\lambda_j k_B T}{\hbar} [|j\rangle \langle j|, \hat{\sigma}(\vec{n}_{j-}, t)] + \lambda_j \gamma_j [|j\rangle \langle j|, \hat{\sigma}(\vec{n}_{j-}, t)]. \quad (20)$$

The ranks of the auxiliary operators continue to infinity, which is impossible to treat computationally. In order to terminate the hierarchically coupled master equations, we set the higher rank operators of $N_{\text{rank}} \geq N_{\text{cutoff}}$ to be zero, *i.e.* $\hat{\sigma}(\vec{n}, t) = 0$ for \vec{n} satisfying $N_{\text{rank}} \geq N_{\text{cutoff}}$. In numerical simulations, this means we increase N_{cutoff} until the dynamics of the reduced electronic state show convergence. In this work, we take $N_{\text{cutoff}} = 10$ in the simulations of Figs. 4 and S6.

We note that the hierarchically coupled master equations in Eq. (18) are different from those in Ref. [2], where local phonon baths were considered. The local bath model corresponds to the case that $s_j = 0$ for all j where the effective Hamiltonian of the electronic states of molecules $\hat{H}_e^{\text{eff}}(t)$ is reduced to the original Hamiltonian \hat{H}_e as the time-dependent Lamb shift vanishes.

SECTION II. PARAMETERS USED IN SIMULATIONS

Here we provide values for the parameters used in the simulations.

Dynamic resonance induced by a shared phonon mode

In Fig. 1, we consider a two-molecule system with $N = 2$ and take the initial single-exciton state $|I\rangle$ as being in a pure state $|1\rangle$ where molecule 1 is excited and molecule 2 is in its electronic ground state. In Fig. 1(a), we take 1) $(\Omega_1 - \Omega_2)/J_{12} = 0$ (no

electronic energy mismatch between molecules), and 2) $f_1 = f_2 = 0$ (no interaction between molecules and phonon mode). In Figs. 1(b)-(d), we take 1) $(\Omega_1 - \Omega_2)/J_{12} = 2$ (electronic energy mismatch), 2) $\omega/J_{12} = 1$, $f_1/J_{12} = 1$ and $f_2/J_{12} = 2$ – here the dipolar coupling J_{12} is small in magnitude compared to the electronic energy mismatch, which would lead to non-resonance of exciton transfer if the shared phonon mode was not coupled to the molecules.

In Fig. S1, we consider a three-molecule system with $N = 3$ and take the initial single-exciton state $|I\rangle$ as being in a pure state $|1\rangle$. We take 1) $J_{12} = J_{23} \equiv J$ and $J_{13} = 0$ (a linear chain), 2) $(\Omega_2 - \Omega_1)/J = 3$ and $(\Omega_3 - \Omega_1)/J = 1$ (a rugged uphill electronic energy landscape, $\Omega_2 > \Omega_3 > \Omega_1$), implying that molecule 2 is an energetic barrier and molecules 1 and 3 are nonresonant. In Fig. S1(a), we take $f_1 = f_2 = f_3 = 0$ (no interaction between molecules and phonon mode). In Fig. S1(b), we take $\omega/J = 1$, $f_1/J = 2.11$, $f_2/J = 2.80$ and $f_3/J = 2.56$.

In Figs. 2 and S2, we consider a two-molecule system with $N = 2$ and take 1) $\omega/J_{12} = 2.4$, 2) $(\Omega_1 - \Omega_2)/J_{12} = 2$, 3) $f_1/J_{12} = -0.5$ and $f_2/J_{12} = 1$. In Figs. 2(a) and S2(a), we take the initial single-exciton state as being in a pure state $|I\rangle = |1\rangle$ where molecule 1 is excited and molecule 2 is in its electronic ground state. In Figs. 2(b) and S2(b), on the other hand, we take $|I\rangle = |2\rangle$ where molecule 2 is excited instead.

In Fig. S3, we consider a two-molecule system with $N = 2$ and take 1) $\omega/J_{12} = 0.143$, 2) $(\Omega_1 - \Omega_2)/J_{12} = -2.14$, 3) $f_1/J_{12} = -0.857$ and $f_2/J_{12} = 0.143$. In Fig. S3(a), we take the initial single-exciton state $|I\rangle = |1\rangle$, whereas in Fig. S3(b), we take $|I\rangle = |2\rangle$.

In Fig. S4, we consider a three-molecule linear chain, with $N = 3$, $J_{12} = J_{23} \equiv J$ and $J_{13} = 0$, and take 1) $(\Omega_1 - \Omega_3)/J = 4$ and $(\Omega_2 - \Omega_3)/J = 2$ (a downhill electronic energy landscape), 2) $\omega/J = 2.29$, $f_1/J = -0.975$, $f_2/J = 0.654$ and $f_3/J = -0.654$. In Figs. S4(b)-(d), we take the initial single-exciton state as being in a pure state $|I\rangle = |1\rangle$, $|I\rangle = |2\rangle$ and $|I\rangle = |3\rangle$, respectively.

In Figs. 3 and S5, we consider a seven-molecule linear chain, with $N = 7$, $J_{jk} \equiv J$ if $j = k \pm 1$ and $J_{jk} = 0$ otherwise, and take the initial single-exciton state $|I\rangle = |1\rangle$. In Figs. 3(a) and S5(b), we take 1) $(\Omega_j - \Omega_k)/J = 0$ for all j and k (a flat electronic energy landscape), and 2) $f_j = 0$ for all j (no interaction between molecules and phonon mode). In Figs. 3(b) and S5(d), we take 1) $(\Omega_1 - \Omega_7)/J = 1.93$, $(\Omega_2 - \Omega_7)/J = 2.06$, $(\Omega_3 - \Omega_7)/J = 2.11$, $(\Omega_4 - \Omega_7)/J = 2.13$, $(\Omega_5 - \Omega_7)/J = 2.14$, $(\Omega_6 - \Omega_7)/J = 2.05$, 2) $\omega/J = 1$, $f_1/J = -0.471$, $f_2/J = -0.305$, $f_3/J = -0.221$, $f_4/J = -0.151$, $f_5/J = 0.129$, $f_6/J = 0.325$ and $f_7/J = 1.47$.

Dynamic resonance induced by a shared phonon bath

In Figs. 4 and S6, we consider a seven-molecule linear chain with $N = 7$, $J_{jk} \equiv J$ if $j = k \pm 1$ and $J_{jk} = 0$ otherwise, and take the initial single-exciton state as being in a pure state $\hat{\rho}_e(0) = |1\rangle\langle 1|$. In Figs. 4(a) and S6(c), we take 1) $(\Omega_j - \Omega_k)/J = 0$ for all j and k (a flat electronic energy landscape), 2) $\lambda_j/J = 0.35$, $\gamma_j/J = 0.35$, $k_B T/\hbar J = 2$ and $s_j = 0$ for all j (local phonon baths). In Figs. 4(b) and S6(d), we take 1) $(\Omega_j - \Omega_{j+1})/J = 2$ (a downhill electronic energy landscape), 2) $\lambda_j/J = 0.35$, $\gamma_j/J = 0.35$, $k_B T/\hbar J = 2$ and $s_j = 0$ for all j (local phonon baths). In Figs. 4(c) and S6(e), we take 1) $(\Omega_j - \Omega_{j+1})/J = 2$ (a downhill electronic energy landscape), 2) $\lambda_j/J = 0.35$, $\gamma_j/J = 0.35$, $k_B T/\hbar J = 2$ and $s_j = j \times (k_B T/\hbar \lambda_j)$ (a shared phonon bath).

* Electronic address: m.tame@imperial.ac.uk

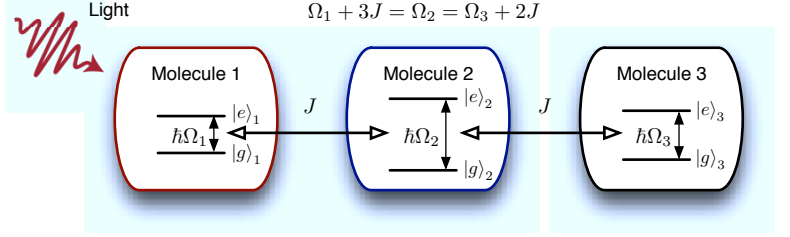
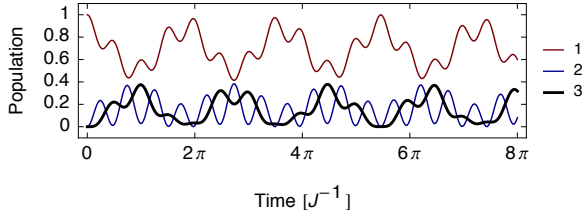
† Electronic address: hyoung@hanyang.ac.kr

[1] N. Makri and D. E. Makarov, J. Chem. Phys. **102**, 4600 (1995).

[2] A. Ishizaki and G. R. Fleming, J. Chem. Phys. **130**, 234111 (2009).

[3] R. P. Feynman and F. L. Vernon, Ann. Phys. **24**, 118 (1963).

(a) Rugged electronic energy landscape (no shared phonon)



(b) Rugged electronic energy landscape (shared phonon)

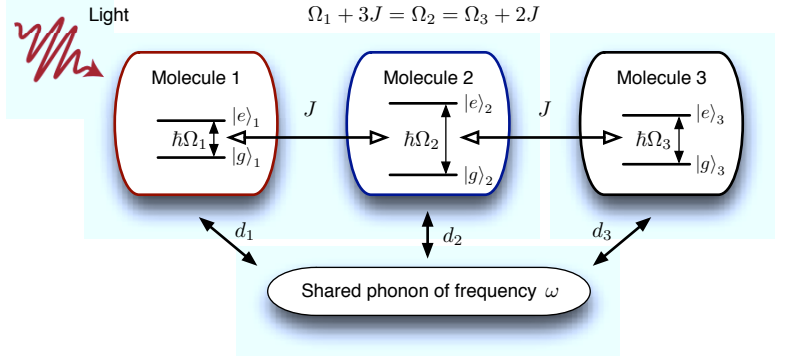
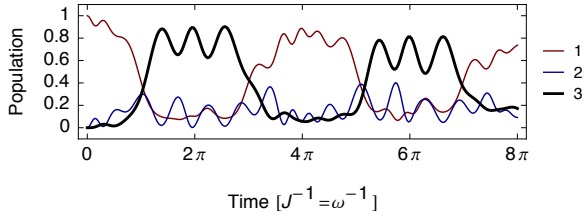
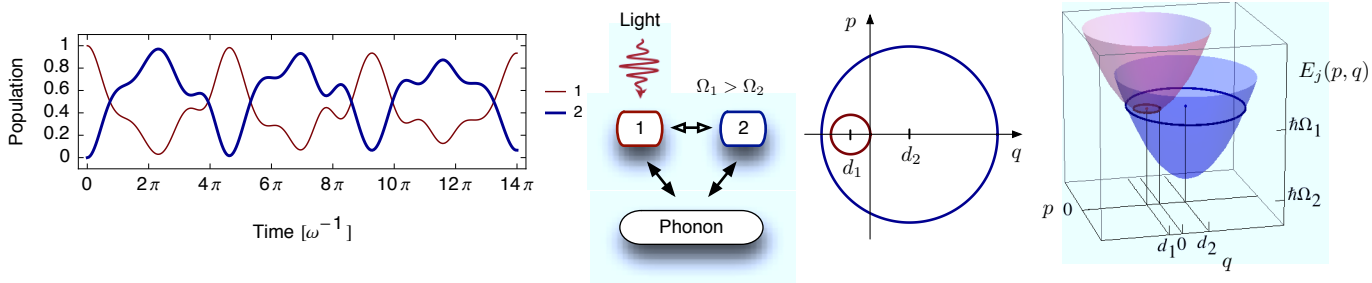


FIG. S 1: Energy transfer through a rugged uphill electronic energy landscape mediated by reversible exchange of energy between exciton and phonon. (a) In the absence of a shared phonon, an exciton is localized at the initial molecule in a rugged landscape due to the non-resonance arising from the energy-level mismatches between initial molecule 1 and the other molecules. Here, a rugged uphill electronic energy landscape $\Omega_2 > \Omega_3 > \Omega_1$ is considered, where the energy-level mismatches are similar in magnitude to the dipolar couplings J between the molecules. (b) In the presence of a shared phonon, an exciton can be efficiently transferred through the rugged landscape. When the exciton hops from low energy molecule 1 to high energy molecule 2, the electronic energy is increased ($\Omega_1 < \Omega_2$), while the potential energy of the phonon is decreased $\frac{1}{2}m\omega^2(q - d_1)^2 > \frac{1}{2}m\omega^2(q - d_2)^2$ due to the change of the equilibrium position of the phonon mode ($d_1 \rightarrow d_2$). In an opposite way, when the exciton hops from high energy molecule 2 to low energy molecule 3, the electronic energy is decreased ($\Omega_2 > \Omega_3$), while the potential energy of the phonon is increased. With energy conservation satisfied, quantum coherence then enables a unidirectional exciton transfer from molecule 1 to 3, such that the exciton stays at molecule 3 for a while with a high probability.

(a) Dynamic resonance energy transfer from high to low energy molecule



(b) Non-resonant energy transfer from low to high energy molecule

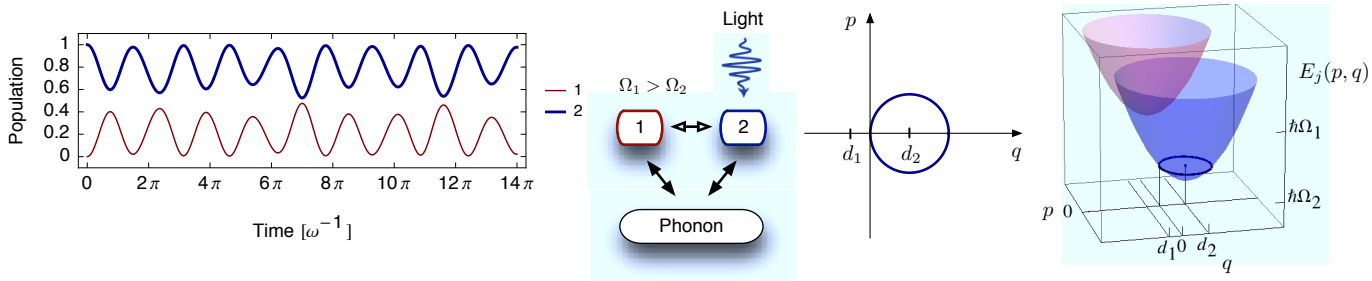
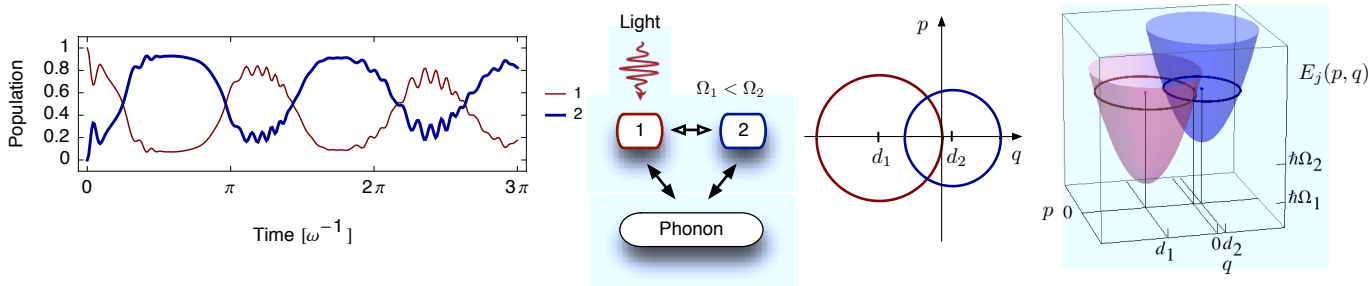


FIG. S 2: Directionality of downhill energy transfer induced by dynamic resonance. Fig. 2 is displayed in detail with the excitonic polaron energy surface.

(a) Dynamic resonance energy transfer from low to high energy molecule



(b) Non-resonant energy transfer from high to low energy molecule

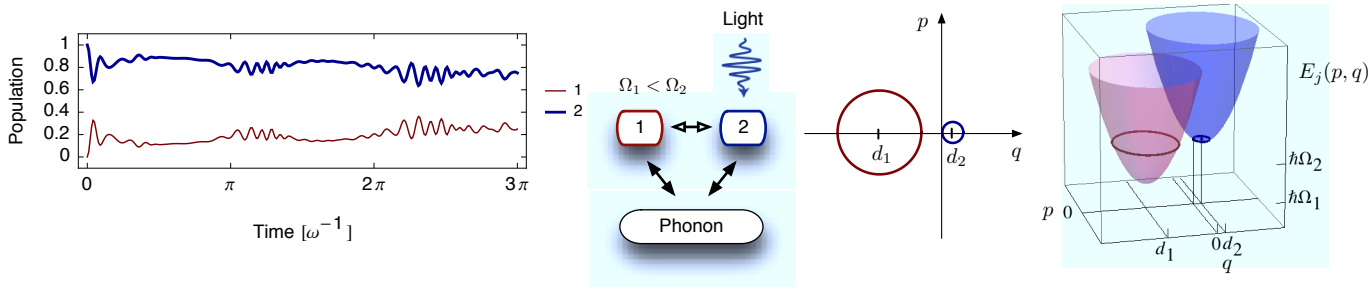
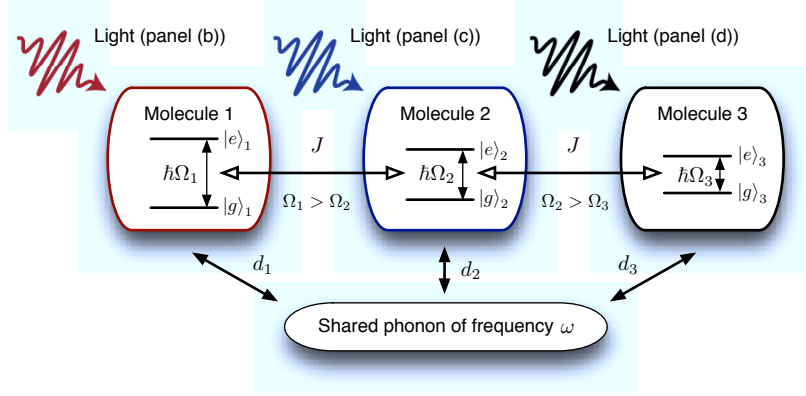
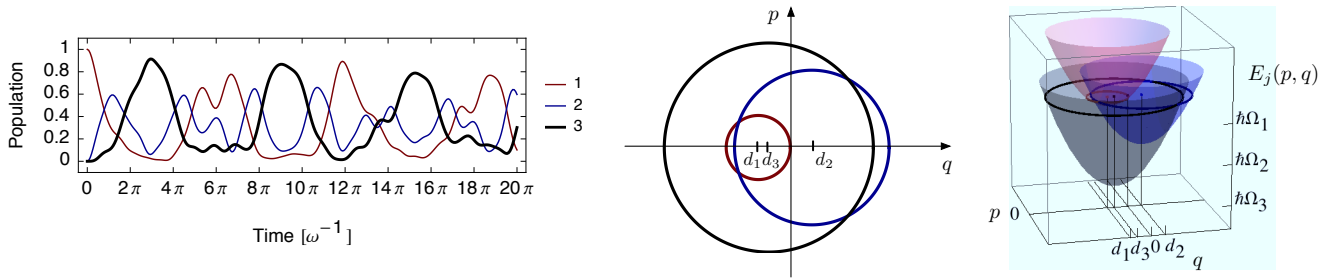


FIG. S 3: Directionality of uphill energy transfer induced by dynamic resonance. Here we consider a two-molecule system with $\Omega_1 < \Omega_2$ where electronic energy of molecule 1 is small in magnitude compared to that of molecule 2. In (a), an exciton created at molecule 1 is transferred from low to high energy molecule by dynamic resonance. In (b), for the same choice of system parameters, an exciton created at molecule 2 is localized at the initial high energy molecule by non-resonance.

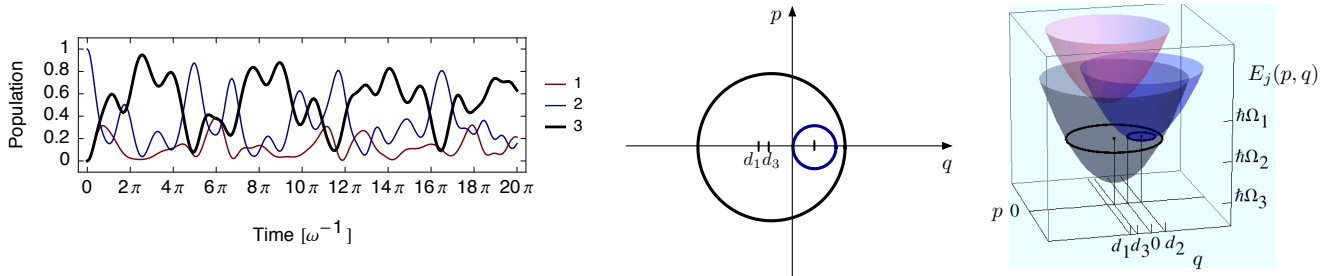
(a) A three-molecule chain coupled to a shared phonon mode



(b) Dynamic resonance energy transfer from molecule 1 to molecule 3



(c) Dynamic resonance energy transfer from molecule 2 to molecule 3 (non-resonance between molecules 1 and 2)



(d) Non-resonant energy transfer from molecule 3 to molecules 1 and 2 (non-resonance between molecule 3 and the other molecules)

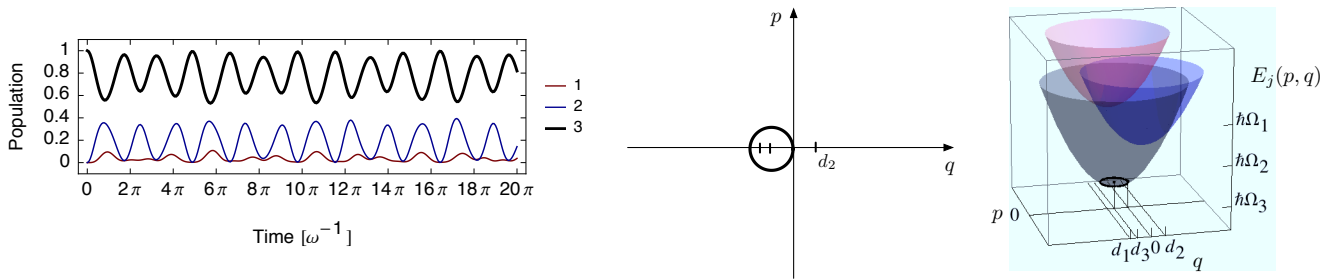


FIG. S 4: Directionality of dynamic resonance energy transfer in a chain of molecules. Here we consider a three-molecule system with a downhill electronic energy landscape, $\Omega_1 > \Omega_2 > \Omega_3$ as shown in (a). In (b), an exciton created at molecule 1 is resonantly transferred from molecule 1 to molecule 3 by dynamic resonance. In (c), an exciton created at molecule 2 is resonantly transferred to molecule 3 by dynamic resonance, while exciton transfer to molecule 1 is suppressed by non-resonance. In (d), an exciton created at molecule 3 is trapped at the initial molecule with high probability due to the non-resonance between molecule 3 and the other molecules.

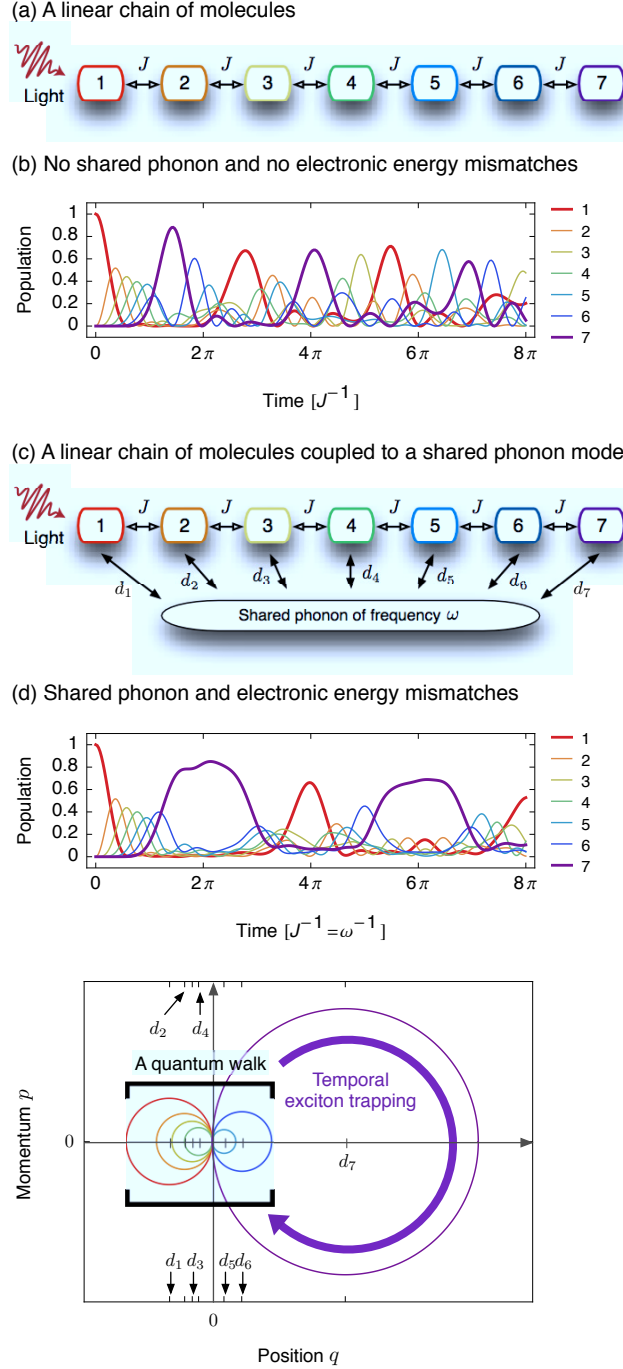
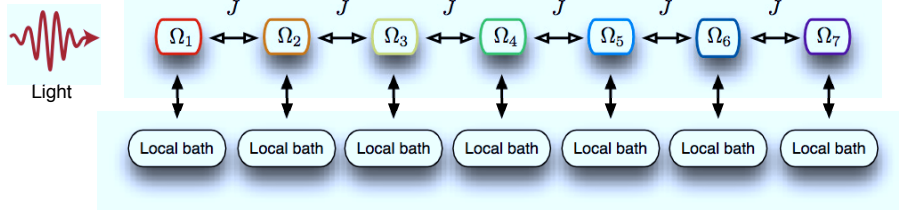
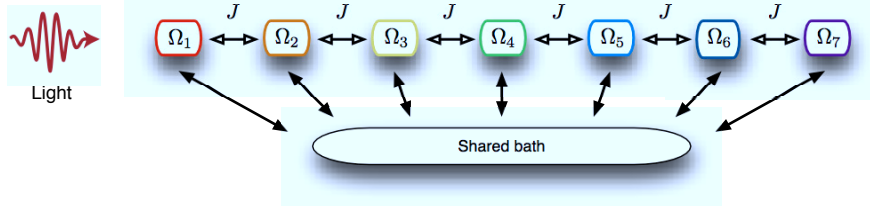


FIG. S 5: Quantum walk and coherent localization induced by a shared phonon mode. In (a), a linear chain of molecules is shown with uniform dipolar couplings J between neighboring molecules. In (b), the dynamics of the populations of the molecules are shown, which leads to the root mean square displacement $\Delta(t) = \sqrt{\langle x^2 \rangle}$ shown in Fig. 3(a). In the absence of electronic energy mismatches, a resonant quantum transition takes place between the molecules. This leads to a quantum walk in a chain of finite size where an exciton is transferred back and forth through the molecules with quantum speed-up due to the reflection at the boundaries of the chain. In (c), a linear chain of molecules is coupled to a shared phonon mode. In (d), the dynamics of the populations of the molecules are shown, which leads to the root mean square displacement $\Delta(t) = \sqrt{\langle x^2 \rangle}$ shown in Fig. 3(b). Even in the presence of electronic energy mismatches, an exciton can be transferred with quantum speed-up by dynamic resonance. When molecule 7, located at one of the boundaries, has the lowest electronic energy, the exciton is temporally trapped at the molecule due to the non-resonance induced by the phonon dynamics. This is a valuable characteristic to have for quantum transport through a chain, for which a source is coupled to one of the boundaries (molecule 1) and a drain (or sink) is coupled to the opposite end (molecule 7). When the internal couplings of the chain, such as the dipolar couplings, are large in magnitude compared to the external coupling between the chain and the drain, the temporal energy trapping at the boundary will enhance unidirectional energy transport from the source to drain by suppressing the reflection at the boundary for a period. This coherence-preserving energy-trapping scheme may also be useful for the transfer of phase information, such as in a quantum state.

(a) A chain of molecules coupled to local phonon baths

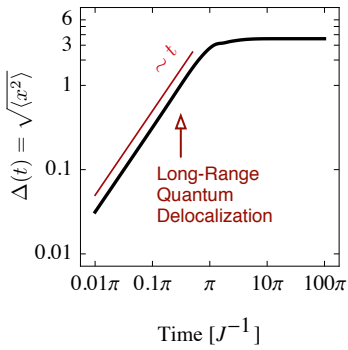
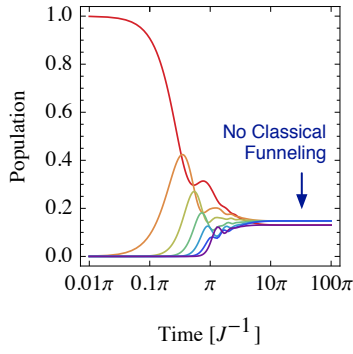


(b) A chain of molecules coupled to a shared phonon bath



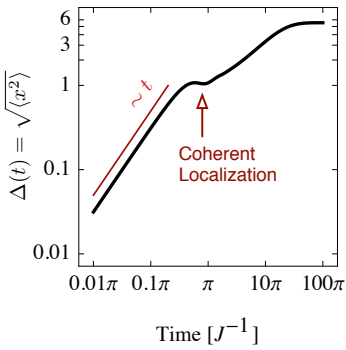
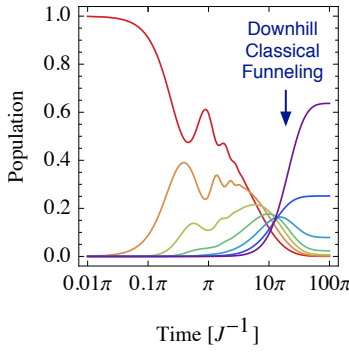
(c) Local phonon bath, flat electronic energy landscape

$$\hbar(\Omega_j - \Omega_{j+1}) = 0$$



(d) Local phonon bath, downhill electronic energy landscape

$$\hbar(\Omega_j - \Omega_{j+1}) = k_B T$$



(e) Shared phonon bath, downhill electronic energy landscape

$$\hbar(\Omega_j - \Omega_{j+1}) = k_B T$$

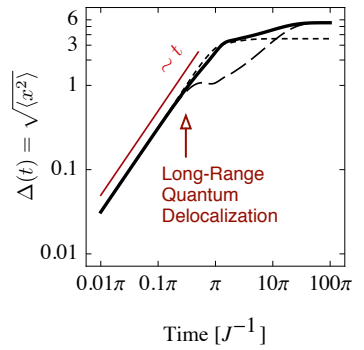
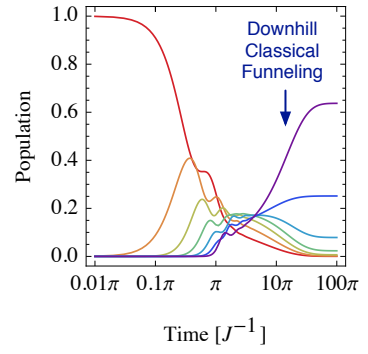


FIG. S 6: Long-range quantum delocalization and classical funneling induced by a shared phonon bath. In (a), a linear chain of molecules is shown, where each molecule is coupled to an independent phonon bath. In (b), a linear chain coupled to a shared phonon bath is shown. In (c)-(e), the dynamics of the populations of the molecules are shown, which correspond to the root mean square displacement $\Delta(t) = \sqrt{\langle x^2 \rangle}$ displayed in Figs. 4(a)-(c), respectively.